



## OPEN

## Luminescence signature of free exciton dissociation and liberated electron transfer across the junction of graphene/GaN hybrid structure

## SUBJECT AREAS:

ULTRAFAST PHOTONICS  
SURFACES, INTERFACES AND  
THIN FILMSReceived  
22 August 2014Accepted  
24 November 2014Published  
8 January 2015Correspondence and  
requests for materials  
should be addressed to  
S.J.X. (sjxu@hku.hk)\* These authors  
contributed equally to  
this work.Jun Wang<sup>1\*</sup>, Changcheng Zheng<sup>1,2\*</sup>, Jiqiang Ning<sup>1</sup>, Lixia Zhang<sup>3</sup>, Wei Li<sup>4,6</sup>, Zhenhua Ni<sup>5</sup>, Yan Chen<sup>6</sup>, Jiannong Wang<sup>3</sup> & Shijie Xu<sup>1</sup>

<sup>1</sup>Department of Physics, HKU-Shenzhen Institute of Research and Innovation (HKU-SIRI), HKU-CAS Joint Laboratory on New Materials, The University of Hong Kong, Pokfulam Road, Hong Kong, China, <sup>2</sup>Mathematics and Physics Centre, Department of Mathematical Sciences, Xi'an Jiaotong-Liverpool University, Suzhou 215123, China, <sup>3</sup>Department of Physics, The Hong Kong University of Science and Technology, Clear Water Bay, Hong Kong, China, <sup>4</sup>State Key Laboratory of Functional Materials for Informatics and Shanghai Center for Superconductivity, Shanghai Institute of Microsystem and Information Technology, Chinese Academy of Sciences, Shanghai 200050, China, <sup>5</sup>Department of Physics, Southeast University, Nanjing 211189, China, <sup>6</sup>Department of Physics, State Key Laboratory of Surface Physics and Laboratory of Advanced Materials, Fudan University, Shanghai 200433, China.

Large-area graphene grown on Cu foil with chemical vapor deposition was transferred onto intentionally undoped GaN epilayer to form a graphene/GaN Schottky junction. Optical spectroscopic techniques including steady-state and time-resolved photoluminescence (PL) were employed to investigate the electron transfer between graphene and n-type GaN at different temperatures. By comparing the near-band-edge excitonic emissions before and after the graphene covering, some structures in the excitonic PL spectra are found to show interesting changes. In particular, a distinct “dip” structure is found to develop at the center of the free exciton emission peak as the temperature goes up. A mechanism that the first dissociation of some freely moveable excitons at the interface was followed by transfer of liberated electrons over the junction barrier is proposed to interpret the appearance and development of the “dip” structure. The formation and evolution process of this “dip” structure can be well resolved from the measured time-resolved PL spectra. First-principles simulations provide clear evidence of finite electron transfer at the interface between graphene and GaN.

Since its first successful exfoliation from bulk graphite and isolated existence in nature<sup>1</sup>, graphene has drawn intensive research interest from scientists in the areas of physics, materials science, chemistry, engineering, etc., due to its excellent electric, mechanic and thermal properties<sup>2,3</sup>, and also due to numerous potential applications in optoelectronic devices, electronic devices, solar cells, phototransistor etc<sup>4-7</sup>. Very recently, particular effort has been devoted to the investigation of integrating graphene with semiconductors, especially GaN, for possible improvements of performance of existing devices and even exploring new schemes<sup>6,8-11</sup>. It is well known that as a technologically important wide band gap semiconductor, GaN has tremendous applications in various fields such as short-wavelength light emitting diodes and lasing diodes, high-temperature and high-power electronic devices etc<sup>12,13</sup>. Previous research about graphene/GaN hybrid structure has been mainly concentrated on the electric/electronic properties<sup>8,14-16</sup>, while few works have been devoted to the photoelectric properties of the composite<sup>17</sup>. In terms of the technological importance of both GaN and graphene in different areas, the optical properties of graphene/GaN hybrid structures are of broad interest due to their unique physical and chemical properties. In this article, we present a detailed study of the optical properties of graphene/GaN hybrid structure at different temperatures by using steady-state and time-resolved photoluminescence (PL) techniques. We observe the luminescence signature of free exciton dissociation and electron transfer over the Schottky barrier of graphene/GaN hybrid structure. Moreover, we find that the efficiency of this two-step carrier process is dependent on the kinetic energy of movable excitons created in the GaN side.

In order to verify layer number and also homogeneousness of the graphene layer, the Raman spectra and image of the graphene/GaN hybrid structure were measured. The micro-Raman scanning images of the 2D mode of

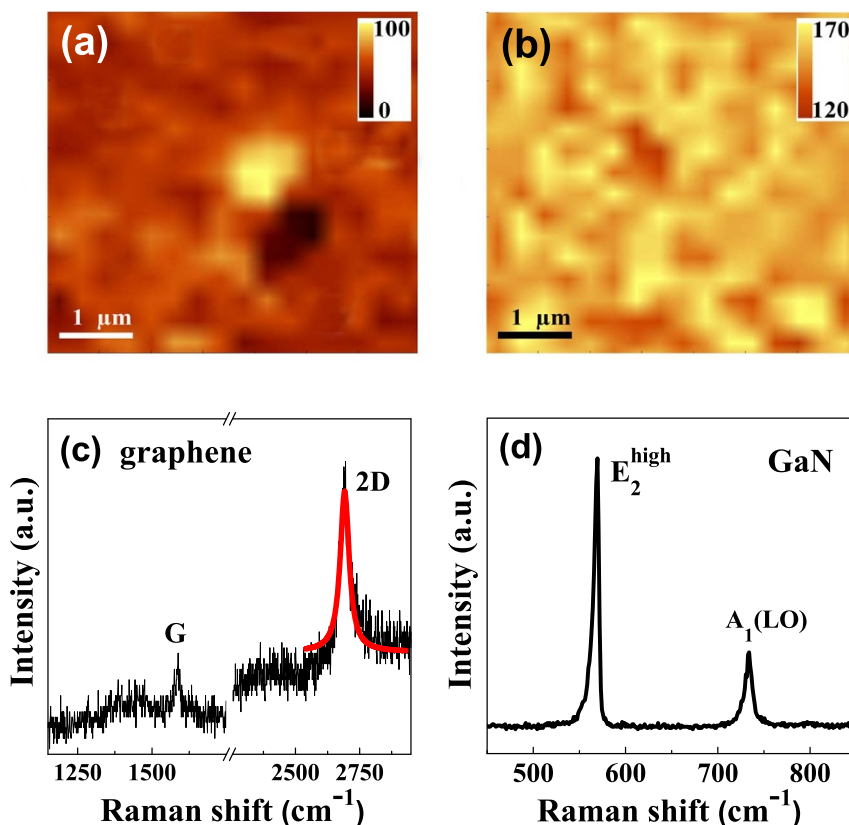


**Figure 1** | Micro-Raman scanning images with an area of  $5 \times 5$  measured from the graphene/GaN hybrid structure. (a) Integrated from the intensity of 2D Raman mode of graphene. (b) Integrated from the intensity of  $E_2^{\text{high}}$  Raman mode of GaN. (c) and (d) Representative Raman spectra extracted from 1(a) and 1(b), respectively.

graphene layer and the  $E_2^{\text{high}}$  Raman mode of GaN were shown in Fig. 1(a) and 1(b), respectively. As can be seen from Fig. 1(a), the graphene studied here was reasonably uniform in terms of its 2D mode intensity. The Raman spectra extracted from a randomly selected point in the images of Fig. 1(a) and 1(b) were depicted in Fig. 1(c) and 1(d), respectively. The two prominent Raman modes of single-layer graphene (G band:  $\sim 1586 \text{ cm}^{-1}$  and 2D band:  $\sim 2690 \text{ cm}^{-1}$ ) can be well resolved in Fig. 1(c). Their intensity ratio,  $I_{2D}/I_G > 2$ , indicates good quality of graphene layer<sup>18,19</sup>. Moreover, the 2D band can be fitted quite well with a Lorentzian lineshape function<sup>19</sup>, as shown in Fig. 1(c). The defect-induced D band ( $\sim 1350 \text{ cm}^{-1}$ ) of graphene is not well resolved probably due to the significant overlapping with the second-order Raman scattering from the underlying GaN epilayer. Compared with the mechanical exfoliated graphene on  $\text{SiO}_2/\text{Si}$  substrate, the 2D band in the graphene/GaN hybrid structure shows a slight blueshift of  $8 \text{ cm}^{-1}$ . Such shift could be due to the joint effects of substrate and preparation technique<sup>18</sup>. The Raman features of the underlying GaN layer keep unchanged except some intensity reduction, compared with the as-grown GaN epilayer (results not shown here). This is due to reflection and absorbance of some incident laser photons.

For graphene/GaN contacts, usually a Schottky junction forms due to van der Waals attraction and electron transfer<sup>6,14,15,17</sup>. Fig. 2(a) and (b) show schematic drawings of band structures of graphene and n-type GaN before and after their contacting, respectively.  $q\phi_g$  is the work function of graphene ( $\sim 4.9 \text{ eV}$  for CVD sample),  $\chi_e$  is the electron affinity of GaN ( $\sim 4.1 \text{ eV}$ ),  $q\phi_{\text{SBH}} \approx 0.74 \text{ eV}$  is Schottky barrier height of graphene/GaN junction<sup>14</sup>.  $V_{bi}$  is the built-in voltage.  $E_g$  is the band gap of GaN and  $E_f$  is the Fermi energy of GaN. As mentioned earlier, the electrical properties of graphene/GaN contact have been addressed previously. In the present work, we concentrate on its optical properties, especially luminescence signatures of free

exciton dissociation at the interface and transfer of liberated electrons over the junction.

PL spectra of the graphene/GaN hybrid structure and the as-grown GaN epilayer measured under the same conditions were depicted in Fig. 2(c) for a temperature range of 1.5–77 K. Since donor bound exciton (denoted by DX) line is almost unaffected by the graphene capping layer, the PL spectra were thus normalized at the intensity of DX peak to make a clear comparison. It can be seen that the  $I_x$  band (a bound exciton with undetermined origin) of the GaN epilayer is significantly weakened after the graphene layer is capped. Moreover, it attenuates faster with increasing temperature in the graphene/GaN sample compared with the case of the bare GaN. In the literature<sup>20</sup>, a similar sharp peak was observed, which is believed to be identical to  $I_x$  emission in this work. However, its origin is still a controversy issue<sup>20–23</sup>. Considering that the intensity of  $I_x$  band can be significantly reduced after the top graphene covering and its fast attenuating with increasing temperatures, we could tentatively ascribe  $I_x$  to the excitons bound at a surface acceptor-like defect which has strong sensitivity to surface environment change.

In addition to the significant reduction and quick thermal quenching of  $I_x$  line, more interesting behavior was observed for free exciton emissions. As can be seen from Fig. 2(c) and Fig. 3, free exciton A ( $\text{FX}_A$ ) bands of the two samples behave very differently as the temperature increases. For the as-grown GaN epilayer,  $\text{FX}_A$  peak gradually becomes dominant due to thermal liberation of bound excitons into free excitons as previously observed<sup>24</sup>. Its lineshape keeps unchanged except broadening due to phonon scattering effect. As for the graphene/GaN hybrid structure, however, the lineshape of the  $\text{FX}_A$  peak shows a remarkable change when temperature is beyond 30 K. A dip at peak center develops and becomes noticeable for temperatures above 77 K. Furthermore, free exciton B ( $\text{FX}_B$ ) emission band also exhibits similar behavior although its intensity is

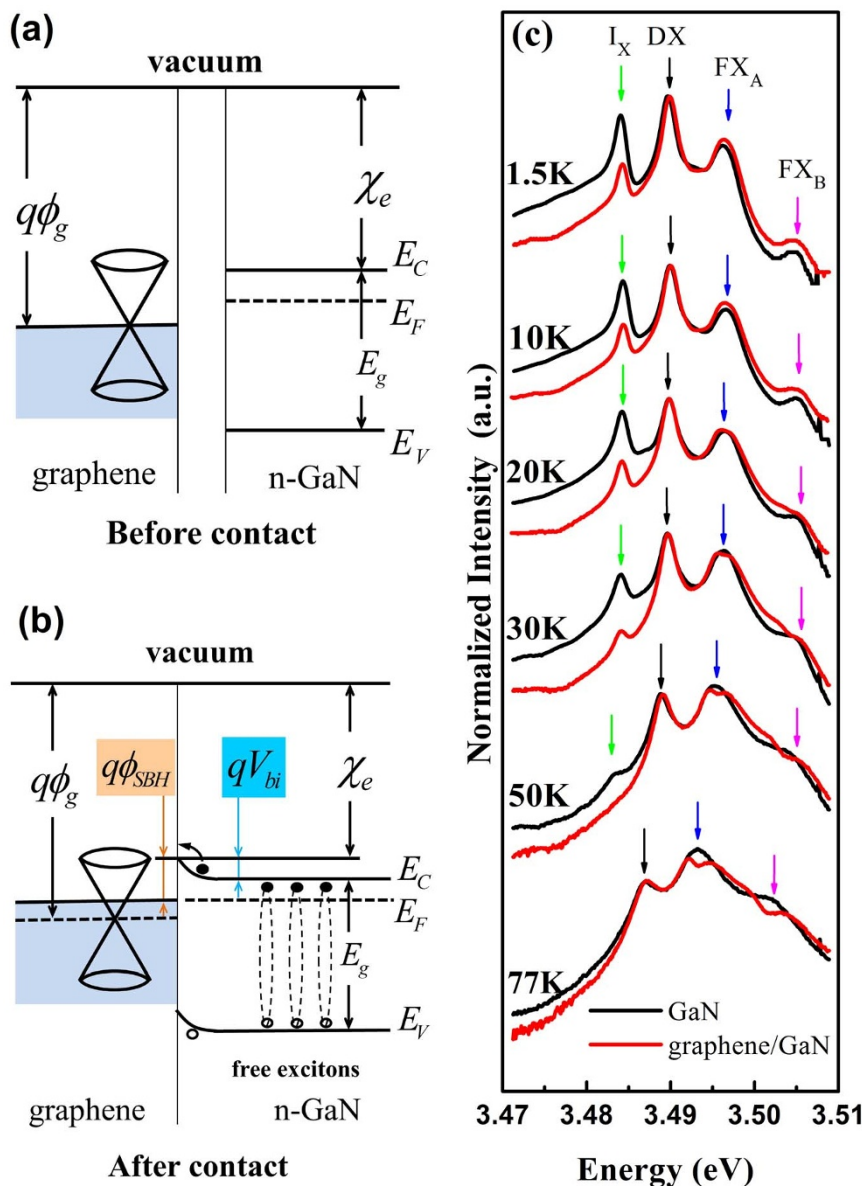


**Figure 2** | Schematic drawings of energy band structures of graphene and n-type GaN before (a) and after the contacting (b). Temperature-dependent PL spectra of the as-grown GaN (black solid line) and graphene/GaN (red solid line) are depicted in semi-logarithmic scale (c). All spectra are normalized at DX peak intensity. DX,  $I_X$ ,  $FX_A$ , and  $FX_B$  lines can be well resolved and indicated by different color vertical arrows.

relatively much weaker. These results reveal that the graphene capping layer has a strong influence on free excitons in the GaN underlying layer.

In order to understand this phenomenon, electronic coupling and charge transfer between graphene and GaN need to be considered<sup>6,15</sup>. Owing to its zero band gap, graphene is usually regarded as a semi-metal and once in touch with semiconductors would exhibit metal-like functions in metal/semiconductor junction. For graphene/GaN, a Schottky junction usually forms at the interface with a Schottky barrier height ( $q\phi_{SBH}$ )<sup>6</sup>. Before contact, neutral single-layer graphene (idealized) has the Fermi level aligned with Dirac points where the occupied branch (bottom) and unoccupied branch (upper) touch to one another, as schematically displayed in Fig. 2(a). Besides, the density of states (DOS) in graphene shows a low and linear dispersion with zero DOS at Dirac points. After paving onto GaN, graphene sheet may take electrons from GaN since as-grown intentionally undoped GaN is n-type conductivity. The electron flow-in could raise graphene's Fermi level during the pinning of the Fermi level in the entire hybrid structure. As a result, a Schottky contact with

rectifying characteristics forms, as schematically shown in Fig. 2(b). Consequently, a narrow depletion layer emerges in the side of GaN layer near the interface with the establishment of a built-in field  $V_{bi}$ . Such contact, in particular the built-in electric field may have a strong impact on the surface related properties of GaN, such as freely moveable excitons and surface defects. Since the laser wavelength 325 nm used in this study is in ultraviolet region, efficient photon absorption occurs within only a very shallow range of about hundred nm underneath the GaN surface due to the large absorption coefficient. In other words, the efficient photon absorption mainly takes place near and within the thin depletion layer in which a built-in electric field already established due to the electron transfer from GaN to graphene in the hybrid structure. In such circumstances, excitons generated in the  $\sim 100$  nm thick layer of GaN near the interface may be significantly affected by graphene and some optical signatures of the effects could be observed.

It is known that free and bound excitons form chronologically within a short time after the excitation in wide band gap semiconductors at low temperatures<sup>25</sup>. For free excitons, they are movable

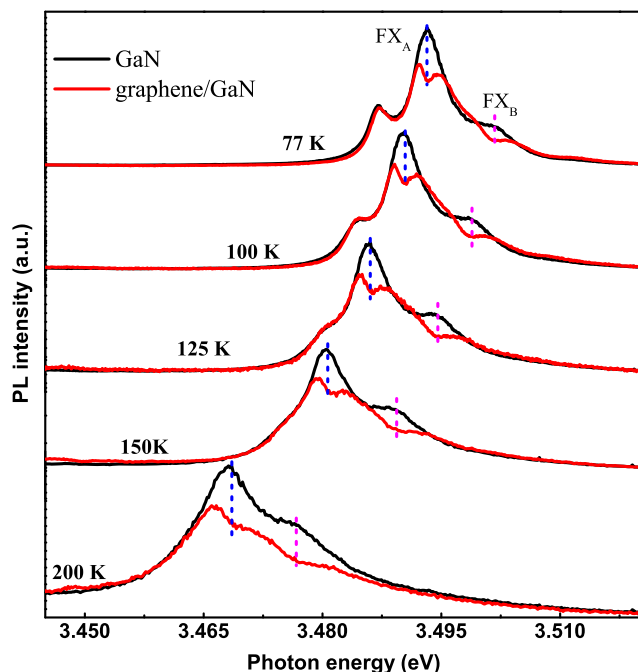


**Figure 3** | Temperature-dependent PL spectra of the as-grown GaN (black) and graphene/GaN hybrid structure (red) from 77 K to 200 K. Dashed blue and magenta lines align with the centers of  $FX_A$  and  $FX_B$  bands, respectively.

and have high probability to arrive at crystal/air interface (surface) where they can annihilate in ways of either radiative recombination or destroyed by surface defects/states. In the former process, light emission occurs. The latter is non-radiative process, and may lead to some reduction in emission intensity or particular features in spectral lineshape by competing with the former process. Therefore, free excitons could be sensitive to the surface environment variation. For bound excitons, such as excitons bound at impurities inside crystal, they are fixed at particular locations, especially at low temperatures. They are thus insensitive to the surface circumstance change except the case of excitons bound at surface defects. Bound excitons usually have much larger oscillator strength than free excitons and thus their emission band is usually dominant over free excitons at low temperatures. Furthermore, they randomly distribute over a much wider interior region in crystal, for example, in GaN.

In the graphene/GaN hybrid structure studied in the present work, a particular attention will be thus paid on free excitons and their PL spectral features. As observed in the PL spectra at different temperatures, on one hand, free exciton emission line such as  $FX_A$  quickly becomes dominant in the PL spectra with increasing temperature due to the efficient thermalization of donor bound excitons into free excitons. On the other hand, kinetic energy of free excitons will increase with increasing temperature. Without doubt, increase in kinetic energy can raise the arriving probability of free excitons at the interface where they may recombine radiatively or get dissociated. Owing to the existence of a graphene layer, some of free excitons arriving at the interface may be dissociated since the semi-metallic graphene selectively captures electrons. Of course, those broken excitons will no longer contribute to the light emission. It is known that in light emission of excitons, conservation principles of both energy and momentum should be obeyed. Compulsorily restricted by principle of momentum conservation, only free excitons with almost zero momentum (i.e., located in the vicinity of the zone center in  $k$  space.) are “bright” excitons contributing to emission due to extremely small momentum of photons. Some of these free excitons with almost zero momentum arrive at the interface and

non-radiatively decomposed into electrons and holes, causing the observed “dip” structures at the spectral centers of  $FX_A$  and  $FX_B$  bands.

In order to obtain a deeper insight into the formation of “dip” structures, time-resolved PL spectra of the graphene/GaN hybrid sample and the as-grown GaN were measured. The results at 77 K were depicted in Fig. 4. It is perfectly clear that appearance and evolution of the dip structures can be seen. Before 180 ps delay time after the femtosecond pulse excitation, the “dip” structures don’t emerge, suggesting that transport of free excitons to the interface and dissociation there don’t efficiently occur within 180 ps. When the delay time was 293 ps the dip structure can be clearly seen. The average transport + dissociation time of free excitons is thus estimated to be 110 ps. As the delay time further increases, the dip structures develop and become more noticeable. In sharp contrast to the case of the hybrid structure, the bare as-grown GaN sample shows normal time-resolved PL spectra. Regarding the peak intensity evolution of  $FX_A$  band with the delay time, luminescence time constants show a significant reduction for the hybrid structure, i.e., from  $\sim 300$  ps of the bare sample to  $\sim 150$  ps of the hybrid structure.

At last, the first-principles simulations on electronic structures of bare GaN and graphene/GaN heterostructure were performed by using the pseudopotential-based code VASP within the Perdew-Burke-Ernzerhof generalized gradient approximation<sup>26,27</sup>, where we use a substrate GaN supercell of size  $2 \times 2 \times 8$ . Throughout the theoretical calculations, a 400 eV cutoff in the plane wave expansion and a  $6 \times 6 \times 1$  Gamma  $k$  grid are chosen to ensure the calculation with an accuracy of  $10^{-5}$  eV. The lattice constants are taken from the experimental values, while the internal atomic positions are optimized until the largest force on each atom was 0.005 eV/Å. As shown in the left panel of Fig. 5, the carbon atoms of graphene couple tightly with the outermost layer of nitrogen atoms so that finite electron transfer may occur in between graphene and GaN. The right panel of Fig. 5 depicts the calculated total density of states (DOS) of bare GaN and graphene/GaN hybrid structure, respectively. Clearly, a significant change in total DOS can be seen before and after graphene contacting with GaN, especially in the free exciton ( $\sim 3.495$  eV) luminescence region. The value of charges transferred from graphene to substrate GaN is estimated to be 0.02e per carbon atom. Our theoretical results show good agreement with experiment and confirm the picture of free exciton dissociation and transfer of liberated electrons.

To conclude, an interesting “dip” structure was observed on the PL spectra of free excitons in graphene/GaN hybrid structure. Its development was also found to be dependent on temperature. Such dip structure is interpreted as a result of free exciton dissociation and transfer of liberated electrons at the interface between graphene and GaN. Time evolution of the “dip” structure was clearly seen via measuring time-resolved PL spectra. The first-principles calculations confirm the physical picture of free exciton dissociation and electron transfer at the interface between graphene and GaN.

## Experimental section

Intentionally undoped GaN epilayer ( $\sim 4 \mu\text{m}$ ) was grown on sapphire substrate by metal-organic chemical vapor deposition (CVD). The carrier concentration in this n-type GaN was estimated as  $5.02 \times 10^{15} \text{ cm}^{-3}$  from the room-temperature Hall measurement. The GaN epilayer was cut into a few pieces (with size of a few millimeters). One piece served as a control sample while others were covered with graphene. Large-area single-layer graphene sheets were synthesized by CVD method on Cu foils (diameter: 25  $\mu\text{m}$ ) at 1000 °C with a flow of  $\text{H}_2$  (40 sccm) and  $\text{CH}_4$  (60 sccm) for 15 min under the pressure of 160 Pa. After 15 min of growth, the sample was cooled down to room temperature in  $\text{H}_2$  atmosphere. After the growth of graphene, the Cu foils were covered with a layer of poly (methyl methacrylate, PMMA). The Cu substrates were then etched in an aqueous iron



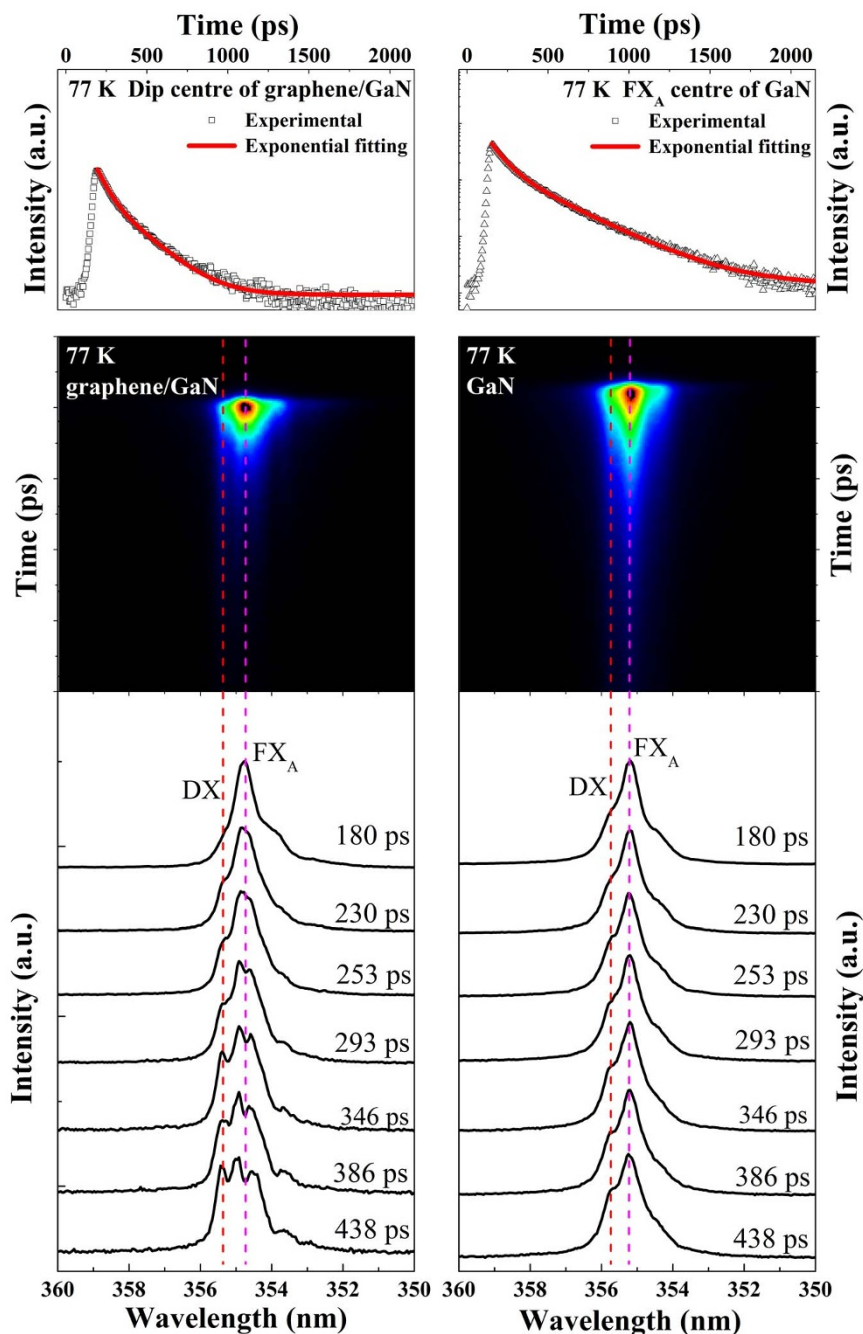


**Figure 4** | Time-resolved PL results of the graphene/GaN (left) and as-grown GaN (right) at 77 K: Decay curves of  $FX_A$  center (top), time-resolved PL images (mid) and time evolutionary PL spectra (bottom). The two vertical lines mark the spectral center positions of  $FX_A$  and  $DX$ , respectively. In the images (mid), the emission signal intensity increases as the image color goes from blue, green, to red.

chloride ( $FeCl_3$ ) solution, leaving the graphene/PMMA film which was washed in deionized water for three times to achieve an aqueous environment with negligible ions for preparation of transfer onto GaN surface. Before the transfer step, the GaN epilayer pieces were cleaned using typical surface-cleaning techniques. It should be mentioned that new graphene growth routes have been very recently developed, which did not require metal catalyst etching or hazardous chemicals at lower temperature<sup>28,29</sup>.

Optical spectral measurements were carried out on the graphene/GaN hybrid structure and the as-grown GaN epilayer piece for comparison. The Raman scattering measurements were taken under the back-scattering geometric configuration on a WITec-Alpha confocal Raman microscope system using the 514.5 nm  $Ar^+$  laser with an

excitation power of  $\sim 1$  mW as the excitation source. In the variable-temperature photoluminescence (PL) measurements, the samples were loaded on the cold finger of the cryostat of a 7 Tesla Spectromag system (Oxford Instruments Nanoscience) with varying temperature from 1.46 K to 300 K. The samples were excited by the 325 nm line from a He-Cd Laser (Kimmon) with output power of 35 mW. The PL signals were dispersed by an ultra-high-resolution monochromator (McPHERSON 20621) equipped with a photomultiplier. Standard lock-in amplifier technique was used to improve the signal-to-noise ratio. In the time-resolved PL (TRPL) measurements, the samples were loaded on the cold finger of a closed cryostat providing a varying temperature from 20 K to 300 K. The excitation source was the 266.7 nm laser pulses (pulse width  $\sim 100$  fs)

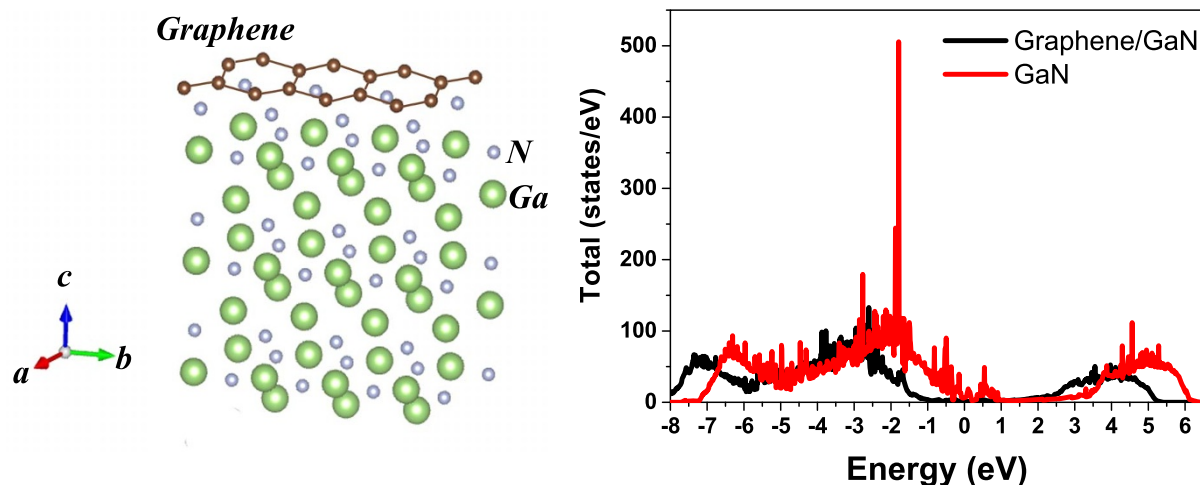


**Figure 5** | The schematic slab hybrid structure of the graphene/GaN (Left Panel) and the calculated total density of states (DOS) for bare GaN and graphene/GaN hybrid structure (Right Panel). Significant change in DOS can be seen in the GaN band gap ( $\sim 3.495$  eV) energy region before and after the graphene covering.

generated from a frequency tripled mode-locked Ti: sapphire oscillator with a repetition rate of 76 MHz. The details of the experimental arrangements have been described elsewhere<sup>25</sup>.

- Novoselov, S. K. *et al.* Electric field effect in atomically thin carbon films. *Science* **306**, 666–669 (2004).
- Balandin, A. A. *et al.* Superior thermal conductivity of single-layer graphene. *Nano Lett.* **8**, 902–907 (2008).
- Castro Neto, A. H., Guinea, F., Peres, N. M. R., Novoselov, K. S. & Geim, A. K. The electronic properties of graphene. *Rev. Mod. Phys.* **81**, 109–162 (2009).
- Wang, X., Zhi, L. J. & Mullen, K. Transparent, conductive graphene electrodes for dye-sensitized solar cells. *Nano Lett.* **8**, 323–327 (2008).
- Bae, S. *et al.* Roll-to-roll production of 30-inch graphene films for transparent electrodes. *Nature Nanotech.* **5**, 574–578 (2010).
- Tongay, S. *et al.* Rectification at Graphene-Semiconductor Interfaces: Zero-Gap Semiconductor-Based Diodes. *Phys. Rev. X* **2**, 011002 (2012).
- Chang, H. X. & Wu, H. K. Graphene-Based Nanomaterials: Synthesis, Properties, and Optical and Optoelectronic Applications. *Adv. Funct. Mater.* **23**, 1984–1997 (2012).
- Wang, L. C. *et al.* Interface and transport properties of GaN/graphene junction in GaN-based LEDs. *J. Phys. D: Appl. Phys.* **45**, 505102 (2012).
- Chang, C. W. *et al.* Graphene/SiO<sub>2</sub>/p-GaN Diodes: An Advanced Economical Alternative for Electrically Tunable Light Emitters. *Adv. Funct. Mater.* **23**, 4043–4048 (2013).
- Wang, L. C. *et al.* Improved transport properties of graphene/GaN junctions in GaN-based vertical light emitting diodes by acid doping. *RSC Adv.* **3**, 3359–3364 (2013).
- Lai, W.-C. *et al.* GaN-based light-emitting diodes with graphene/indium tin oxide transparent layer. *Opt. Express* **22**, A396–A401 (2014).
- Morkoc, A. H. *Nitride Semiconductors and Devices*. (Springer, Berlin, 1999).
- Nakamura, S., Fasol, G. & Pearton, S. J. *The Blue Laser Diodes* (Springer, Berlin, 2000).
- Tongay, S. *et al.* Graphene/GaN Schottky diodes: Stability at elevated temperatures. *Appl. Phys. Lett.* **99**, 102102 (2011).
- Zhong, H. J. *et al.* Self-adaptive electronic contact between graphene and semiconductors. *Appl. Phys. Lett.* **100**, 122108 (2012).
- Nepal, N. *et al.* Epitaxial Growth of III-Nitride/Graphene Heterostructures for Electronic Devices. *Appl. Phys. Express* **6**, 061003 (2013).
- Lin, F. *et al.* Graphene/GaN diodes for ultraviolet and visible photodetectors. *Appl. Phys. Lett.* **105**, 073103 (2014).
- Ni, Z. H., Wang, Y. Y., Yu, T. & Shen, Z. X. Raman Spectroscopy and Imaging of Graphene. *Nano Res.* **1**, 273–291 (2008).
- Ferrari, A. C. *et al.* Raman spectrum of graphene and graphene layers. *Phys. Rev. Lett.* **97**, 187401 (2006).
- Monemar, B. *et al.* Recombination of free and bound excitons in GaN. *Phys. Status Solidi (b)* **254**, 1723–1740 (2008).
- Kornitzer, K. *et al.* Photoluminescence and reflectance spectroscopy of excitonic transitions in high-quality homoepitaxial GaN films. *Phys. Rev. B* **60**, 1471 (1999).
- Pozina, G., Bergman, J., Paskova, T. & Monemar, B. Bound exciton dynamics in GaN grown by hydride vapor-phase epitaxy. *Appl. Phys. Lett.* **75**, 4124–4126 (1999).

- Fischer, S. *et al.* Shallow donors in epitaxial GaN. *Mater. Sci. & Engineer. B* **43**, 192–195 (1997).
- Xu, S. J., Liu, W. & Li, M. F. Direct determination of free exciton binding energy from phonon-assisted luminescence spectra in GaN epilayers. *Appl. Phys. Lett.* **81**, 2959–2961 (2002).
- Zheng, C. C. *et al.* Formation dynamics of excitons and temporal behaviors of Fano resonance due to the exciton-impurity-phonon configuration interaction in ZnO. *J. Phys. Chem. A* **116**, 381–385 (2012).
- Kresse, G. & Furthmüller, J. Efficient iterative schemes for ab initio total-energy calculations using a plane-wave basis set. *Phys. Rev. B* **54**, 11169 (1996).
- Perdew, J. P., Burke, K. & Ernzerhof, M. Generalized Gradient Approximation Made Simple. *Phys. Rev. Lett.* **77**, 3865 (1996).
- Ostrikova, K., Neytsb, E. C. & Meyyappanc, M. Plasma nanoscience: from nanosolids in plasmas to nano-plasmas in solids. *Adv. Phys.* **62**, 113–224 (2013).
- Kumar, S., van der Laan, T., Rider, A. E., Randeniya, L. & Ostrikov, K. Multifunctional Three-Dimensional T-Junction Graphene Micro-Wells: Energy-Efficient, Plasma-Enabled Growth and Instant Water-Based Transfer for Flexible Device Applications. *Adv. Funct. Mater.* **24**, 6114–6122 (2014).

## Acknowledgments

This work was supported by Shenzhen Municipal Science and Technology Innovation Council (Contract No. JCYJ20120615142933076), HK-RGC-GRF Grants (Grant No. HKU 705812P), the University Development Fund and the SRT on New Materials of HKU, and partially by a grant from the University Grants Committee Areas of Excellence Scheme of the Hong Kong Special Administrative Region, China (Project No. [AoE/P-03/08]). CCZ acknowledges partial support from XJTU by RDF-12-02-03. WL and YC were supported by the State Key Programs of China (Grant Nos. 2012CB921604), the National Natural Science Foundation of China (Grant Nos. 11074043 and No. 11274069). JNW wishes to acknowledge the financial support from HK-RGC-GRF Grants (No. 604410).

## Author contributions

W.J., C.C.Z., J.Q.N. and S.J.X. wrote the manuscript. W.J. and C.C.Z. performed the Raman and PL measurements, and also TRPL experiments with help from L.X.Z. and J.N.W. W.L. and Y.C. did the first-principles calculations. Z.H.N. provided the graphene sample and transferred it onto GaN. S.J.X. supervised the project. All the authors discussed the results and reviewed the manuscript.

## Additional information

**Competing financial interests:** The authors declare no competing financial interests.

**How to cite this article:** Wang, J. *et al.* Luminescence signature of free exciton dissociation and liberated electron transfer across the junction of graphene/GaN hybrid structure. *Sci. Rep.* **5**, 7687; DOI:10.1038/srep07687 (2015).



This work is licensed under a Creative Commons Attribution-NonCommercial-NoDerivs 4.0 International License. The images or other third party material in this article are included in the article's Creative Commons license, unless indicated otherwise in the credit line; if the material is not included under the Creative Commons license, users will need to obtain permission from the license holder in order to reproduce the material. To view a copy of this license, visit <http://creativecommons.org/licenses/by-nc-nd/4.0/>